JOURNAL OF AGRICULTURAL AND FOOD CHEMISTRY

Article

pubs.acs.org/JAFC

Assessment of Peeling of *Astragalus* Roots Using ^{1}H NMR- and UPLC-MS-Based Metabolite Profiling

Jee-Youn Jung,[†,‡] Youngae Jung,[†] Jin-Sup Kim,[†,§] Do Hyun Ryu,*[,⊥] and Geum-Sook Hwang*[,†,§]

[†]Integrated Metabolomics Research Group, Seoul Center, Korea Basic Science Institute, Seoul 136-713, Republic of Korea

[‡]KM Health Technology Research Group, Medical Research Division, Korea Institute of Oriental Medicine, Daejeon 305-811, Republic of Korea

[§]Graduate School of Analytical Science and Technology, Chungnam National University, Daejeon 305-764, Republic of Korea

[⊥]Department of Chemistry, Sungkyunkwan University, Suwon 440-746, Republic of Korea

Supporting Information

ABSTRACT: A metabolomic analysis was performed to examine the postharvest processing of *Astragalus membranaceus* roots with a focus on the peeling procedure using ^{1}H NMR and UPLC-MS analyses. Principal component analysis (PCA) score plots from the ^{1}H NMR and UPLC-MS data showed clear separation between peeled and unpeeled *Astragalus* roots. Peeled roots exhibited significant losses of several primary metabolites, including acetate, alanine, arginine, caprate, fumarate, glutamate, histidine, *N*-acetylaspartate, malate, proline, sucrose, trigonelline, and valine. In contrast, the peeled roots contained higher levels of asparagine, aspartate, and xylose, which are xylem-related compounds, and formate, which is produced in response to wound stress incurred during postharvest processing. In addition, the levels of isoflavonoids and astragalosides were significantly reduced in peeled *Astragalus* root. These results demonstrate that metabolite profiling based on a combination of ^{1}H NMR and UPLC-MS analyses can be used to evaluate peeling procedures used in the postharvest processing of herbal medicines.

KEYWORDS: *postharvesting process, plant metabolomics, Astragalus root, quality assessment*

INTRODUCTION

Astragalus membranaceus is used as an herbal medicine with multiple pharmacological effects and is widely cultivated in Korea and China. It has been used as an immunostimulant, tonic, hepatoprotectant, diuretic, antidiabetic analgesic, expectorant, and sedative.[1−4] Generally, *A. membranaceus* roots originating from Korea go through a peeling procedure that includes peeling and drying of *Astragalus* roots below 60 °C for 1 or 2 days, followed by drying under ambient conditions, prior to their release onto the market. *A. membranaceus* root cultivated in China is generally unpeeled and dried.

The peeling procedure commonly used with Korean *Astragalus* roots leaves the roots with a clean, hygienic appearance that yields a sales advantage over unpeeled Chinese *Astragalus* roots. Therefore, two types of commercial products, unpeeled and peeled *Astragalus* roots, which are called "qupi-huangqi" and "pi-huangqi", respectively, circulate in Korean markets, and >80% of them are peeled roots. However, a recent report has stated that peeled *Astragalus* roots (pi-huangqi) exhibit lower antioxidant effects than unpeeled roots (qupi-huangqi).[5] In addition, levels of astragalosides differ considerably among the root components, with the highest concentrations located primarily between the xylem and the bark.[6] Moreover, phloem, which is located just under the bark, carries organic nutrients, whereas the xylem, which is the light yellow part of the proximal portion of the older root containing vessels and xylem fibers, transports water and soluble inorganic ions.[7] Therefore, the peeling process may affect the metabolites contained in extracts of *Astragalus* roots.

The quality of herbs depends highly on the species, geographical origins, cultivation and harvesting methods, and postharvest processing.[8] Such inherent variability emphasizes the importance of metabolite profiling with regard to quality control, formulation, and safe usage of herbal medicines.[9] Recently, metabolite profiling has gained popularity using techniques such as nuclear magnetic resonance (NMR) or liquid chromatography (LC)− or gas chromatography (GC)−mass spectrometry (MS)[9−13] A single analytical method is seldom adequate to sample the large range of metabolites required for a metabolic profiling.[14] Therefore, metabolic profiling requires a multiplatform approach. Such methods have been employed to study other herbal medicines, including *Angelica gigas*, ginseng, and wine.[15−17]

Among the various analytical platforms, ^{1}H NMR is particularly well suited for plant metabolic profiling, allowing detection and quantification in a single measurement of not only abundant primary metabolites but also various groups of secondary metabolites in complex mixtures such as plant extracts. In addition, NMR provides detailed information regarding the quantity and identity of metabolites.[18] LC-MS techniques are fast and highly sensitive. Ultraperformance liquid chromatography−mass spectrometry (UPLC-MS) techniques are capable of rapid, high-capacity analyses, thus facilitating the full analysis of complex samples with diverse chemical characteristics.[19,20] As a result, many studies have emphasized the importance of complementary techniques, such as LC-MS and NMR, in metabolomic studies.[14,18,21]

Received: June 14, 2013
Revised: September 22, 2013
Accepted: September 28, 2013
Published: September 28, 2013

dx.doi.org/10.1021/jf4026103 | J. Agric. Food Chem. 2013, 61, 10398−10407

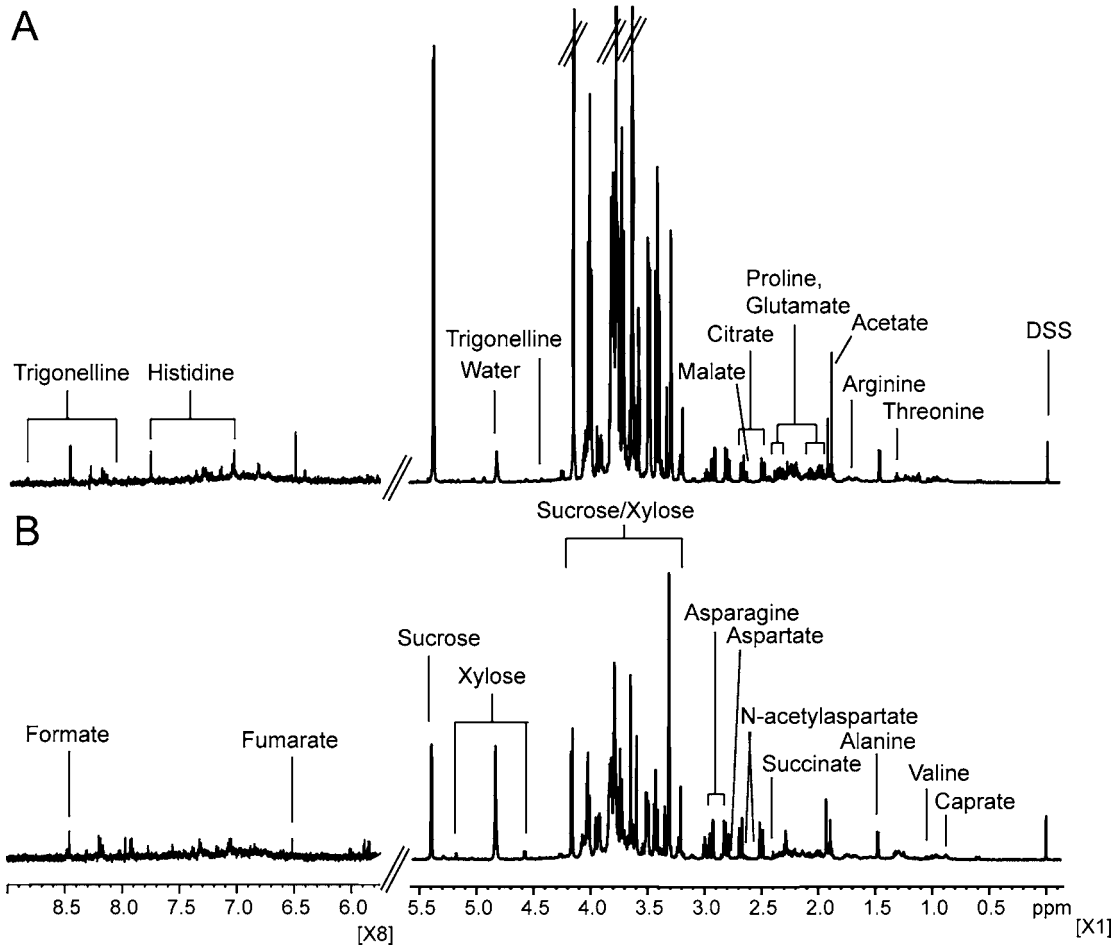

Figure 1. Representative ^{1}H NMR spectra of aqueous extracts of (A) unpeeled (pi-huangqi) and (B) peeled (qupi-huangqi) *Astragalus* roots.

Several metabolomic studies on *Astragalus* roots have focused on the ability to discriminate samples according to geographical origin and species.[6,22] To date, however, there is no metabolomic study that evaluates the effects of postharvest processing on *Astragalus* roots. The current study investigates metabolic variations in *Astragalus* roots as a function of postharvest processing, particularly the peeling procedures, using ^{1}H NMR and UPLC-MS analyses. This study shows that a combination of NMR and UPLC-MS can be used as a reliable approach for obtaining complementary information on primary and secondary metabolites as a function of postharvest processing.

MATERIALS AND METHODS

Plant Material. *A. membranaceus* roots were obtained from Jecheon-si (city), Chungcheongbuk-do (province), South Korea.

Astragalus samples were collected from 18 different gardens within the same geographical region, and two postharvest processing techniques were used on the pool of roots from different plants in the same gardens. Thus, a total of 36 samples were prepared (18 unpeeled *Astragalus* (pi-huangqi) and 18 peeled *Astragalus* (qupi-huangqi)). All of the plant samples were harvested in October and were the same species, which were genetically identical.

After harvesting, all of the samples were allowed to dry under ambient conditions (15−20 °C) for 3 days. Then, half of them were peeled and the rest were not peeled. After the peeling process, all of the samples (peeled and unpeeled) were dried at 40 °C in a dryer for 1 day and stored during the same period at −80 °C.

Chemicals and Authentic Standards Used in UPLC-MS Identification. Methanol-d_4 (99.8%), purchased from Sigma-Aldrich, and deuterium oxide (D_2O, 99.9%), from Cambridge Isotope Laboratories, Inc., were used as NMR solvents. Acetonitrile, methanol, and water (HPLC grade) used in extraction and acquisition for UPLC-MS analysis were purchased from Burdick & Jackson. Formic acid solution (49−51%), 2,2-dimethyl-2-silapentane-5-sulfonic acid (DSS, 97%), bis(2-ethylhexyl) phthalate (BEHP, 99.7%), sodium phosphate dibasic (Na_2HPO_4, 99%), and sodium phosphate monobasic (NaH_2PO_4, 99%) were obtained from Sigma-Aldrich.

To identify the unknown compounds in UPLC-MS experiments, authentic standards of formononetin (≥99.0%) and astragaloside IV (>98.0%) were purchased from Sigma-Aldrich.

Sample Preparation for NMR and UPLC-MS Analyses. Dried *Astragalus* roots were freeze-dried and ground to a fine powder. Five hundred microliters of methanol-d_4 (99.8%), 400 μL of 0.2 M phosphate buffer solution (0.2 M Na_2HPO_4, 0.2 M NaH_2PO_4 in D_2O, pH 7.0), and 100 μL of 5 mM DSS (97%) were added to 100 ± 0.5 mg of dried powder as extraction solvents. D_2O was used for the internal lock signal, and DSS was used as an internal standard with a chemical shift (δ) of 0.0 ppm. Extracts were sonicated for 20 min, followed by centrifugation (10 min, 16609*g*) at room temperature, and adjusted to pH 7.0 ± 0.5 using 1 M NaOH and 1 M HCl. The extract (600 μL) was transferred to 5 mm NMR tubes for NMR analysis.

For UPLC-MS analyses, 2.5 mL of methanol (99.8%), 2.5 mL of water, 20 μL of 0.1 mg/mL DSS, and 15 μL of 0.1 mg/mL bis(2-ethylhexyl) phthalate (BEHP) were added to 50 mg of freeze-dried powder of *Astragalus* roots as extraction solvents. DSS and BEHP were used as internal standards in negative and positive modes, respectively. The sample was mixed for 1 min, sonicated for 20 min, and centrifuged at 2499*g* for 15 min at 25 °C. To exclude impurities, the supernatant was filtered through a 0.22 μm PTFE syringe filter (Merck Millipore, Bedford, MA, USA) and transferred to an autosampler vial. All samples

were prepared and analyzed in random order with respect to class for NMR and UPLC-MS experiments to avoid any bias.

NMR Spectroscopy. ^{1}H NMR spectra were acquired on a VNMRS 600 MHz NMR spectrometer (Agilent Technologies Inc., Santa Clara, CA, USA) using a triple-resonance, 5 mm, HCN salt-tolerant cold probe. ^{1}H NMR spectra were acquired using the NOESY PRESAT pulse sequence, which was applied to suppress signals from residual water. A total of 32 scans were collected into 67568 data points using a spectral width of 8445.9 Hz, a relaxation delay of 2.0 s, an acquisition time of 4.0 s, and a mixing time of 100 ms. A 0.5 Hz line-broadening function was applied to all spectra for Fourier transformation (FT) followed by phasing and baseline correction. Signal assignments for representative samples were achieved using two-dimensional (2D) total correlation spectroscopy (TOCSY), heteronuclear multiple-quantum correlations (HMQC), Chenomx NMR suite 7.1, a 600 MHz (pH 6.0−8.0) NMR database, spiking experiments, and comparison with literature values.[23,24]

UPLC and MS Conditions. Liquid chromatography−electrospray ionization−tandem mass spectrometry LC-ESI-MS/MS analyses of extracts of dried *Astragalus* root were performed using an ultra-performance liquid chromatograph/quadrupole time-of-flight mass spectrometer (UPLC/Q-TOF MS). Analyte separation was conducted through a UPLC system (Acquity UPLC system, Waters, Manchester, UK) equipped with an ethylene-bridged hybrid (BEH) C18 column (100 × 2.1 mm, 1.7 μm particle size) (Waters). The column temperature was constant at 40 °C. Samples on the autosampler were maintained at 10 °C for the duration of these analyses. The injected sample volume was 10 μL using a full loop method. The mobile phase consisted of (A) HPLC grade water with 0.1% formic acid and (B) acetonitrile with 0.1% formic acid. The elution flow rate was 0.45 mL/min. Elution began with a mobile phase of 5% B for 1 min, followed by a linear gradient to 95% B over 6 min. The mobile phase was returned to 5% B for 3 min at the end of each run to equilibrate the separation system for subsequent runs. This UPLC eluate was introduced via an electrospray DuoSpray ion source into a triple TOF 5600 MS/MS system (AB SCIEX, Framingham, MA, USA). For untargeted analysis, total ion chromatograms were acquired using the following operating parameters in both positive and negative modes: capillary voltage, 4500 V; nebulizer pressure, 50 psi; drying gas pressure, 50 psi; curtain gas pressure, 30 psi; source temperature, 500 °C; declustering potential, 70 eV; collision energy, 10 eV.

For targeted analysis, the MRM^{HR} workflow was used to selectively quantify seven secondary metabolites. Because MRM^{HR} lacks the "Q_3" specificity, high-resolution extracted ion chromatograms (XICs) of several fragment ions were generated and integrated. Specific values of collision energy (CE) were used to obtain reliable results. In the positive mode, the CE for calycosin-7-*O*-β-D-glucose, calycosin-7-*O*-β-D-glucoside-6″-*O*-malonate, ononine, calycosin, formononetin, and BEHP (internal standard) were set at 30, 30, 18, 30, 18, and 20 eV, respectively, with an accumulation time of 50 ms. In the negative mode, the CEs for astragaloside IV, astragaloside II, and DSS (internal standard) were set at −40, −50, and −30 eV, respectively, with an accumulation time of 100 ms. The exact mass calibration was performed automatically before each analysis employing the Automated Calibration Delivery System.

^{1}H NMR Data Analysis. All NMR spectra were phase-adjusted and baseline-corrected using Topspin 3.0 and Amix software 3.9.4 (Bruker Biospin, Inc.), respectively.

For untargeted analysis, each NMR spectrum was binned into integrating regions having equal bin sizes of 0.005 ppm over a δ range of 0.75−9.25. All shifts related to the solvent, that is, located between 3.28−3.33 and 4.7−4.90 ppm, and DSS were eliminated. The spectra were then normalized to the total spectral area and exported as a text file for chemometric analysis. The text files were imported into SIMCA-P+ version 12.0 (Umetrics, Umeå, Sweden) for multivariate data analysis and Pareto-scaled to minimize the influence of baseline deviations and noise.[25] Principal component analyses (PCA) were initially performed to examine the intrinsic variation in the data set and to obtain an overview of the variation among groups.

For targeted analysis, metabolites of *Astragalus* roots were quantified using Chenomx NMR suite 7.1 software, which compares the integral of a known reference signal (DSS) with the signal derived from a library of compounds containing chemical shifts and peak multiplicities for all of the resonances of the compound.

Table 1. Chemical Shifts of Metabolites Identified from ^{1}H NMR Analyses of Dried *Astragalus* Root Samples[a]

metabolite	chemical shift (δ)[b]	identification
acetate	1.92 (s)	Chenomx, spiking
alanine	1.47 (d), 3.78 (q)	Chenomx, TOCSY
arginine	1.64 (m), 1.72 (m), 1.90 (m), 3.23 (t), 3.24 (t), 3.76 (t)	Chenomx,TOCSY, HSQC
asparagine	2.82 (dd), 2.94 (dd), 3.94 (q)	Chenomx, TOCSY, HSQC
aspartate	2.64 (dd), 2.8 (d), 3.89 (dd)	Chenomx
caprate	0.85 (t), 1.26 (m), 1.53 (m), 2.2 (t)	Chenomx, TOCSY
citrate	2.54 (d), 2.7 (d)	Chenomx, TOCSY
formate	8.46 (s)	Chenomx, spiking
fumarate	6.53 (s)	Chenomx, spiking
glutamate	2.13 (m), 2.42 (m), 3.71 (dd)	Chenomx, TOCSY
histidine	3.11 (dd), 3.24 (dd), 3.98 (dd), 7.06 (s), 7.78 (s)	Chenomx, spiking,
N-acetyl-aspartate	2.01 (s), 2.49 (dd), 2.68 (dd), 4.38 (m), 7.91 (d)	Chenomx, TOCSY
malate	2.4 (q), 2.7 (dd), 4.3 (d)	Chenomx, TOCSY
proline	1.99 (m), 2.05 (m), 2.36 (m), 3.34 (m), 3.45 (m), 4.12 (m)	Chenomx, TOCSY
succinate	2.47 (s)	Chenomx, spiking
sucrose	3.42 (t), 3.51 (dd), 3.65 (s), 3.73 (t), 3.78 (q), 3.8 (m), 3.81 (m), 3.88 (m), 4.02 (t), 4.16 (t), 5.4 (d)	Chenomx, TOCSY, HSQC
threonine	1.33 (d), 3.61 (d), 4.22 (q)	Chenomx, TOCSY
trigonelline	4.42 (s), 8.07 (t), 8.83 (dd), 9.11 (s)	Chenomx
valine	1.0 (d), 1.05 (d), 2.27 (m), 3.6 (d)	Chenomx, TOCSY
xylose	3.21 (t), 3.30 (t), 3.42 (t), 3.51 (dd), 3.65 (m), 3.92 (dd), 4.6 (d), 5.2 (d)	Chenomx, TOCSY

[a]Concentration was determined by Chenomx 7.1. [b]s, singlet; d, doublet; q, quartet; t, triplet; m, multiplet.

UPLC-MS Data Analysis. Extracts of *Astragalus* root were analyzed to monitor the effect of peeling using a UPLC/Q-TOF MS. Peak finding, peak alignment, and peak filtering of raw data were carried out using MarkerView software version 1.2.1.1 (AB SCIEX). For peak finding, data collection parameters were as follows: subtraction offset, 5 scans; subtraction multiplier, 1.3; minimum spectral peak width, 1 ppm; retention time peak width, 5 scans. For alignment, retention time and mass tolerances were set to 0.5 min and 10 ppm, respectively. For filtering, the intensity threshold was set to 10, and peaks detected in fewer than 2 samples were removed. Peak area matrices normalized by total area were exported to SIMCA-P+ version 12.0 (Umetrics) for multivariate statistical analysis. The intensity of each precursor ion was analyzed by PCA. The details of data analysis are similar to those used with the NMR data.

Relative quantitative analyses of seven secondary metabolites, calycosin-7-*O*-β-D-glucoside-6″-*O*-malonate, calycosin-7-*O*-β-D-glucose, calycosin, ononin, formononetin, and astragalosides II and IV, were executed by dividing the peak area obtained for each analyte by the peak area of the internal standard using MultiQuant software version 2.1(AB SCIEX). This ratio served to correct for instrument/analyst error. Formononetin and astragaloside IV were identified with authentic standards, but others were putatively identified with MS and MS/MS pattern.

Statistical Methods. Student's *t* test was performed using GraphPad PRISM (ver. 5.0; GraphPad Software, Inc.) to test the significance of differences between metabolite levels in *Astragalus* roots subjected to different postharvest processes. The critical *p* value was set to 0.05.

RESULTS AND DISCUSSION

^{1}H NMR Analyses. Proton NMR analyses of two aqueous extracts of dried *Astragalus* roots yielded similar spectroscopic fingerprints with replicate samples of each postharvest process.

Figure 1 shows representative ^{1}H NMR spectra of unpeeled and peeled *Astragalus* roots. Spectral resonances of metabolites were assigned according to spiking experiments, 2D NMR spectra, and the 600- MHz library from Chenomx NMR suite version 7.1. The spectra were dominated by signals corresponding to primary metabolites, including acetate, alanine, arginine, asparagine, aspartate, caprate, citrate, formate, fumarate, glutamate, histidine, *N*-acetylaspartate, malate, proline, succinate, sucrose, threonine, trigonelline, valine, and xylose, and several secondary metabolites, including formononetin and calycosin (Table 1). Primary metabolites are naturally high in plants; thus, secondary metabolites were more difficult to detect than primary metabolites in 1D NMR spectra and were identified by comparisons with the literature,[22,23] spiking experiments, and 2D NMR using TOCSY and HMQC (Supporting Information Figure S1).

The ^{1}H NMR spectra of peeled and unpeeled *Astragalus* roots exhibited significant differences in the carbohydrate region (3.0−4.5 ppm). Unpeeled *Astragalus* roots contained higher levels of histidine and fumarate, whereas the dominant metabolites in the peeled samples were aspartate and asparagine.

Pattern Recognition Analysis of ^{1}H NMR Spectra. PCAs were performed on NMR spectra derived from aqueous extracts of dried *Astragalus* root to assess the intrinsic variations between peeled and unpeeled samples. The PCA score plot in Figure 2

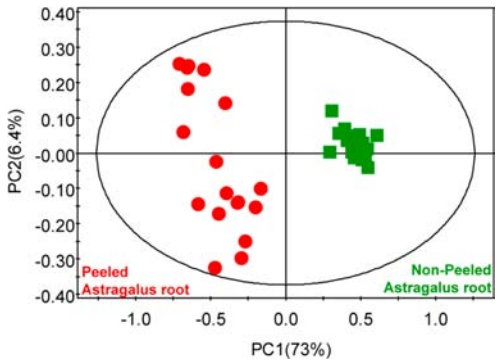

Figure 2. PCA score plot derived from ^{1}H NMR spectra, which mainly included primary metabolites of dried *Astragalus* samples ($R^2X = 0.794$). The symbols represent each sample according to peeling status (green squares, unpeeled *Astragalus* root; red circles, peeled *Astragalus* root).

shows differential clustering according to peel status along the first principal component (R^2X = 0.794). This indicates that peeling affects the patterns of metabolites because the variability of samples projected on the second principal component is mainly due to the difference between sample preparations and is much lower than variability induced by the peeling process.

UPLC-MS Analyses. The exact masses and retention times of individual components from dried *Astragalus* root extracts were measured in both positive and negative ionization modes using an autosampler-equipped UPLC-MS system. Positive ionization mode provided the highest sensitivity and ionization efficiency for isoflavonoids, whereas negative ionization mode was suitable to the astragaloside analyses.

Figure 3, panels A and B, shows base peak chromatograms (BPC) of dried *Astragalus* roots obtained in positive and negative modes, respectively. Chromatograms of more complex samples, however, provided only limited information as multiple analytes eluted simultaneously. Therefore, XICs were used to monitor the detected metabolites. XICs were collected for seven secondary metabolites detected in peeled and unpeeled *Astragalus* root samples (Supporting Information Figures S2 and S3), providing both mass and retention times.

ESI-MS/MS was used to confirm the chemical structure of each component. Five secondary metabolites were detected in positive ionization mode. The mass peak containing a precursor ion peak at m/z 533 with fragment ion peaks at m/z 285 [M + H − malonylglucosyl]$^+$, 270 [M + H − malonylglucosyl − CH_3]$^+$, and 253 [M + H − malonylglucosyl − CH_3 − CH_3OH]$^+$ was putatively identified as calycosin-7-*O*-*β*-D-glucoside-6″-*O*-malonate (Figure 4A). A precursor ion peak at m/z 447 (Figure 4B) with fragment ion peaks at m/z 285 [M + H − glucosyl] $^+$, 270 [M + H − glucosyl − CH_3]$^+$, and 253 [M + H − glucosyl − CH_3 − CH_3OH]$^+$ was matched with the mass pattern of calycosin-7-*O*-*β*-D-glucose. A precursor peak at m/z 285 (Figure 4C) with five fragment ion peaks at 270 [M + H − CH_3] $^+$, 253 [M + H − CH_3OH] $^+$, 225 [M + H − CH_3OH − CO] $^+$, 213 [M + H − CO_2 − CO]$^+$, and 197 [M + H − CH_3OH − 2CO] $^+$ was the same mass pattern as calycosin. The spectra (Figure 4D) yielding a precursor ion peak at m/z 431 with fragment ion peaks at 269 [M + H − glucosyl]$^+$ was matched with ononin. Fomononetin (Figure 4E) yielded a precursor ion peak at m/z 269 with fragment ion peaks at m/z 253 [M + H − CH_3]$^+$, 237 [M + H − CH_3OH]$^+$, 225 [M + H − CO_2]$^+$, 213 [M + H − 2CO]$^+$, 197 [M + H − CO − CO_2]$^+$, and 169 [M + H − CH_3OH − 2CO]$^+$, which confirmed the standard compound.

A peak of astragaloside IV was detected in negative mode (Figure 4F) at m/z 783 [M − H]$^-$ with fragment ion peaks at 489 [M − H − Glu − Xyl]$^-$ and 161 [Glu − H]$^-$. Astragaloside II (Figure 4G) was putatively identified at m/z 825 [M − H]$^-$ with

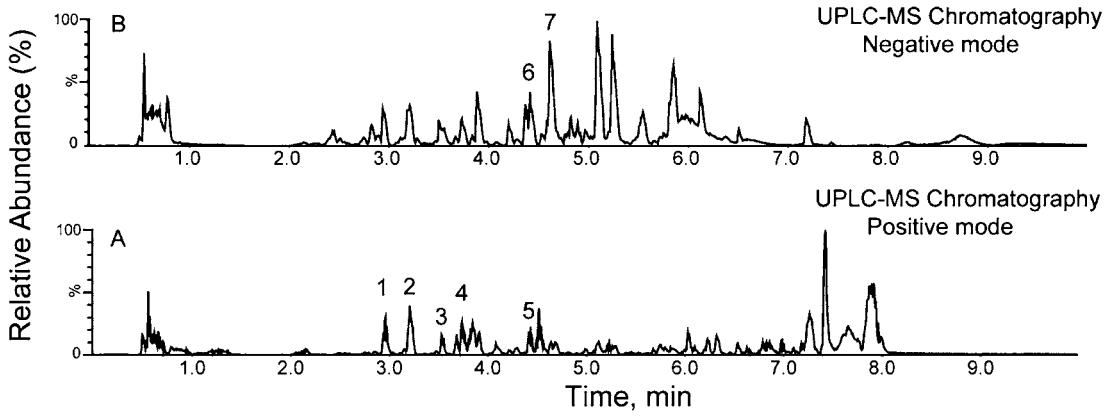

Figure 3. (A) ESI+ and (B) ESI− base peak intensity chromatography (BPC) from a UPLC-MS chromatography of dried *Astragalus* roots (1, calycosin-7-*O*-*β*-D-glucose; 2, calycosin-7-*O*-*β*-D-glucoside-6″-*O*-malonate; 3, ononine; 4, calycosin; 5, formononetine; 6, astragaloside IV; 7, astragaloside II).

dx.doi.org/10.1021/jf4026103 | J. Agric. Food Chem. 2013, 61, 10398−10407

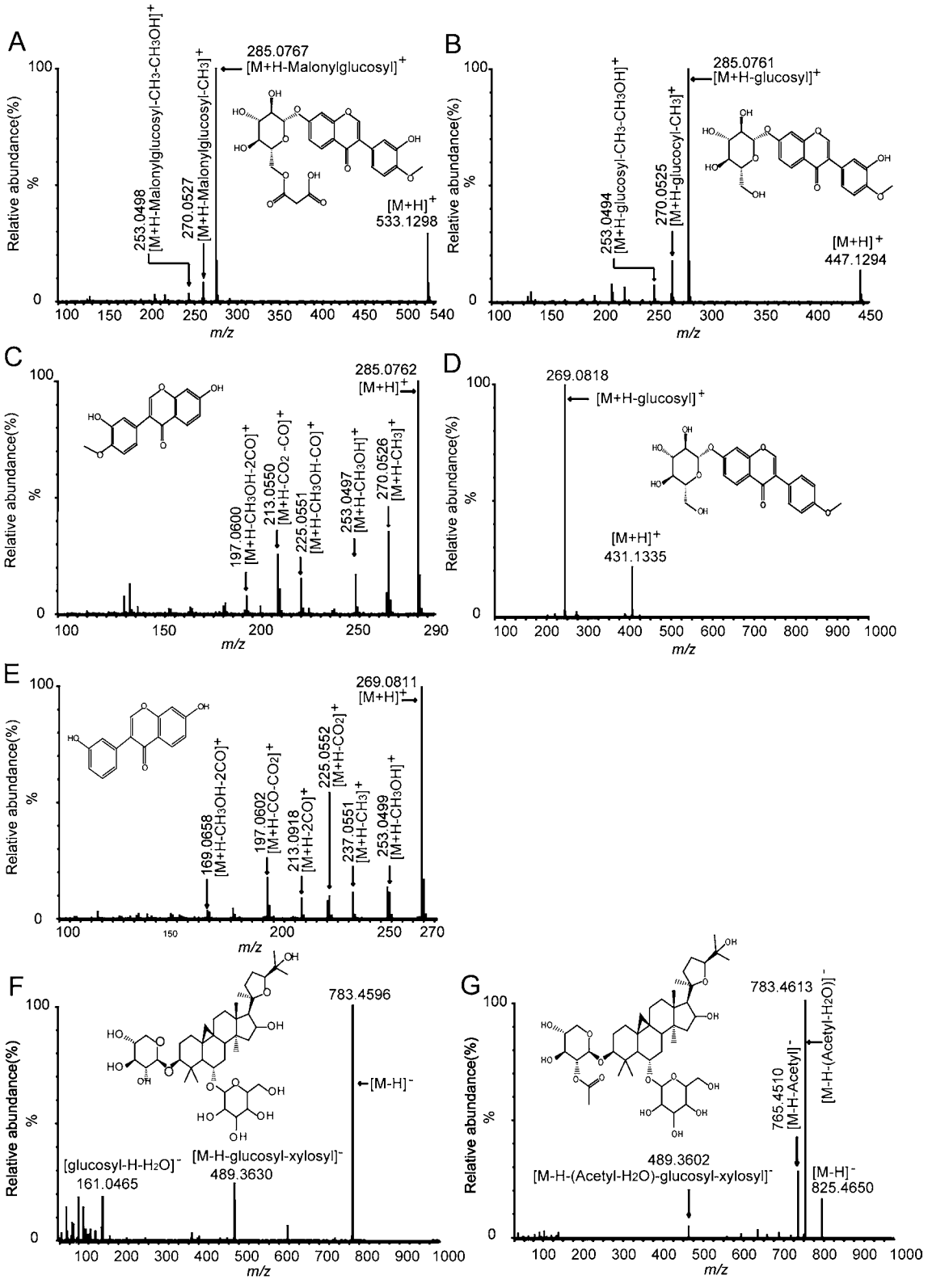

Figure 4. Proposed ion assignments for LC-ESI-MS/MS spectra of (A) calycosin-7-*O*-*β*-D-glucoside-6″-*O*-malonate at *m*/*z* 533, (B) calycosin-7-*O*-*β*-D-glucose at *m*/*z* 447, (C) calycosin at *m*/*z* 285, (D) ononin at *m*/*z* 431, and (E) formononetin at *m*/*z* 269 in positive mode. Fragmentation patterns of (F) astragaloside IV at *m*/*z* 783 and (G) astragaloside II at *m*/*z* 825 were acquired in negative mode.

fragment ion peaks at *m*/*z* 783 $[M - H - (Ac - H_2O)]^-$, 765 $[M - H - Ac]^-$, and 489 $[M - H - (Ac - H_2O) - Glu - Xyl]^-$.

Pattern Recognition Analysis of UPLC-MS Data. PCAs of the untargeted UPLC-MS data were used to create secondary metabolic fingerprints of the peeled and unpeeled *Astragalus* root samples. The PCA score plots derived from positive (Figure 5A) and negative (Figure 5B) modes of the UPLC-MS spectra showed clear separation by peel status (positive, $R^2X = 0.741$; negative, $R^2X = 0.806$).

dx.doi.org/10.1021/jf4026103 | J. Agric. Food Chem. 2013, 61, 10398−10407

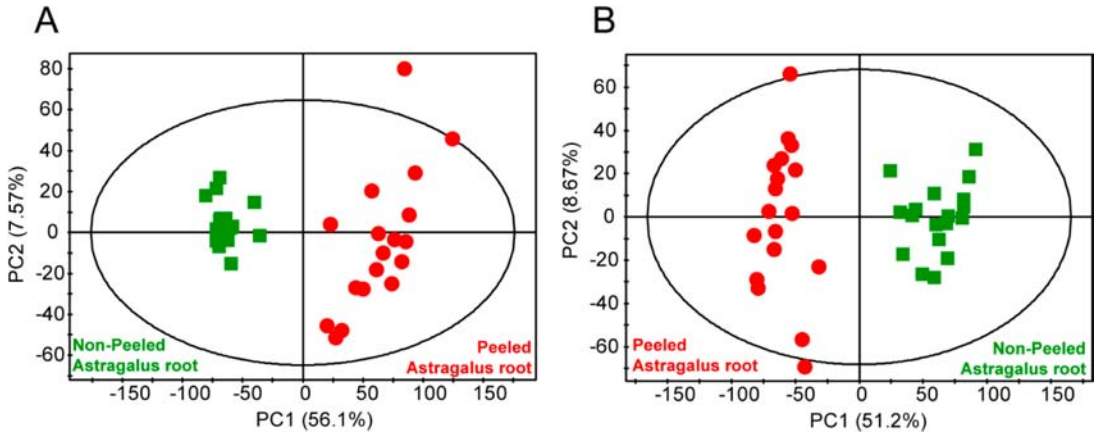

Figure 5. PCA score plots derived from untargeted analysis of UPLC-MS spectra, which maily included secondary metabolites of *Astragalus* samples acquired in (A) positive and (B) negative ionization mode (A, $R^2X = 0.741$; B, $R^2X = 0.806$). Symbols refer to the peel status (green squares, unpeeled *Astragalus* root; red circles, peeled *Astragalus* root).

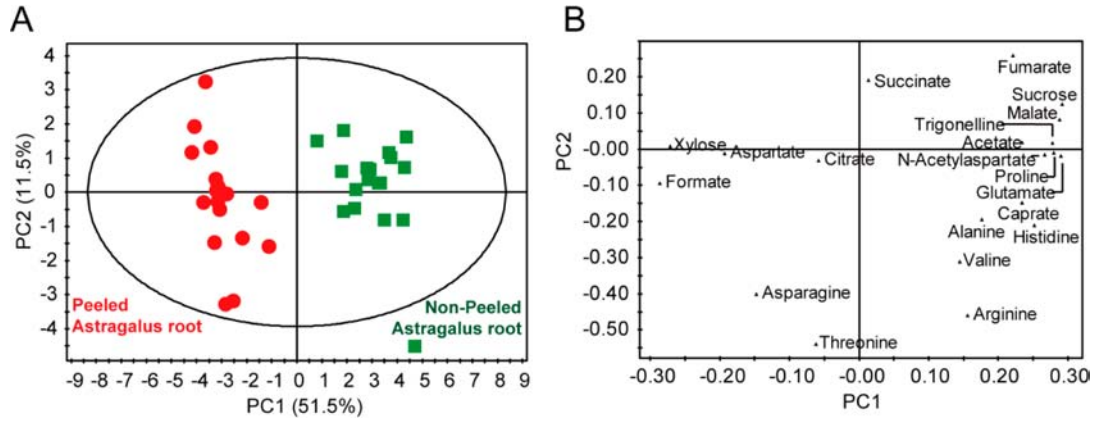

Figure 6. (A) PCA scores and (B) corresponding loading scatter plots derived from targeted profiling of mainly primary metabolites of unpeeled (green squares) and peeled (red circles) *Astragalus* samples ($R^2X = 0.629$). The left and right sides of the loading plot indicate higher levels of metabolites in peeled and unpeeled *Astragalus* samples, respectively.

Target Profiling of Primary Metabolites. To remove the many irrelevant variables and relative greater weight of high-variance variable, such as sucrose, when using Pareto-scaling, and to further our understanding of primary metabolite patterns in *Astragalus* roots, the metabolites previously assigned according to NMR spectra were quantitated. The scatter plot of the PCA of primary metabolites (Figure 6A) shows distinct patterns for peeled and unpeeled *Astragalus* roots ($R^2X = 0.63$). The corresponding loading plot (Figure 6B) reveals that unpeeled *Astragalus* roots are characterized by higher levels of most of the primary metabolites, including acetate, alanine, arginine, caprate, fumarate, glutamate, histidine, *N*-acetylaspartate, malate, proline, sucrose, trigonelline, and valine. In contrast, levels of asparagine, aspartate, xylose, and formate were higher in peeled *Astragalus* roots. Statistically significant differences were observed between the levels of all of these metabolites (Figure 7).

Alteration of Primary Metabolite Levels. By the peeling process, *Astragalus* roots lose their bark but also their weight, up to 86.8%. Therefore, we hypothesized that *Astragalus* roots with intact bark would contain higher levels of most metabolites. In our results, most of the metabolites in bark showed much higher concentrations than those in xylem of unpeeled *Astragalus* root (Supporting Information Figure S4). Especially, essential amino acids, such as arginine, valine, and sucrose, were higher in unpeeled *Astragalus* roots. However, despite the loss of a portion of the root, peeled samples showed higher levels of asparagine, aspartate, formate, and xylose. Moreover, in the distribution ratio of these metabolites and sucrose in bark and xylem from unpeeled astragalus root, asparagine, aspartate, formate, and xylose of xylem showed higher ratios than bark, whereas sucrose showed a higher ratio in bark (Supporting Information Table S1).

There are two transport tissues in vascular plants: xylem, which is located in the plant's interior, and phloem, which is located just under the bark. Peeling *Astragalus* roots likely results in a loss of bark and phloem and exposes the xylem, thereby allowing the xylem content to be more easily extracted. In general, sucrose and amino acids are present at high concentrations in the phloem but are typically at much lower levels in the xylem.[26] In contrast, nitrate (NO_3^-) is typically found at higher levels in the xylem but is not present in the phloem. This is because inorganic nitrogen is assimilated in the roots and transported through the xylem to sites where it is in high demand.[27] Nitrate taken up by mycorrhizal and nonmycorrhizal roots is assimilated primarily into amino compounds by underground tissues.[28] As a result, organic nitrogen compounds and only traces of NO_3^- or NH_4^+ are transported from the roots to the shoots through the xylem.[29−31] Glutamate, glutamine, asparagine, and aspartate are important N-transport compounds and are frequently exchanged between the xylem and phloem. In legumes such as *Astragalus*, glutamate, which converted from glutamine, have been suggested as

dx.doi.org/10.1021/jf4026103 | *J. Agric. Food Chem.* 2013, 61, 10398−10407

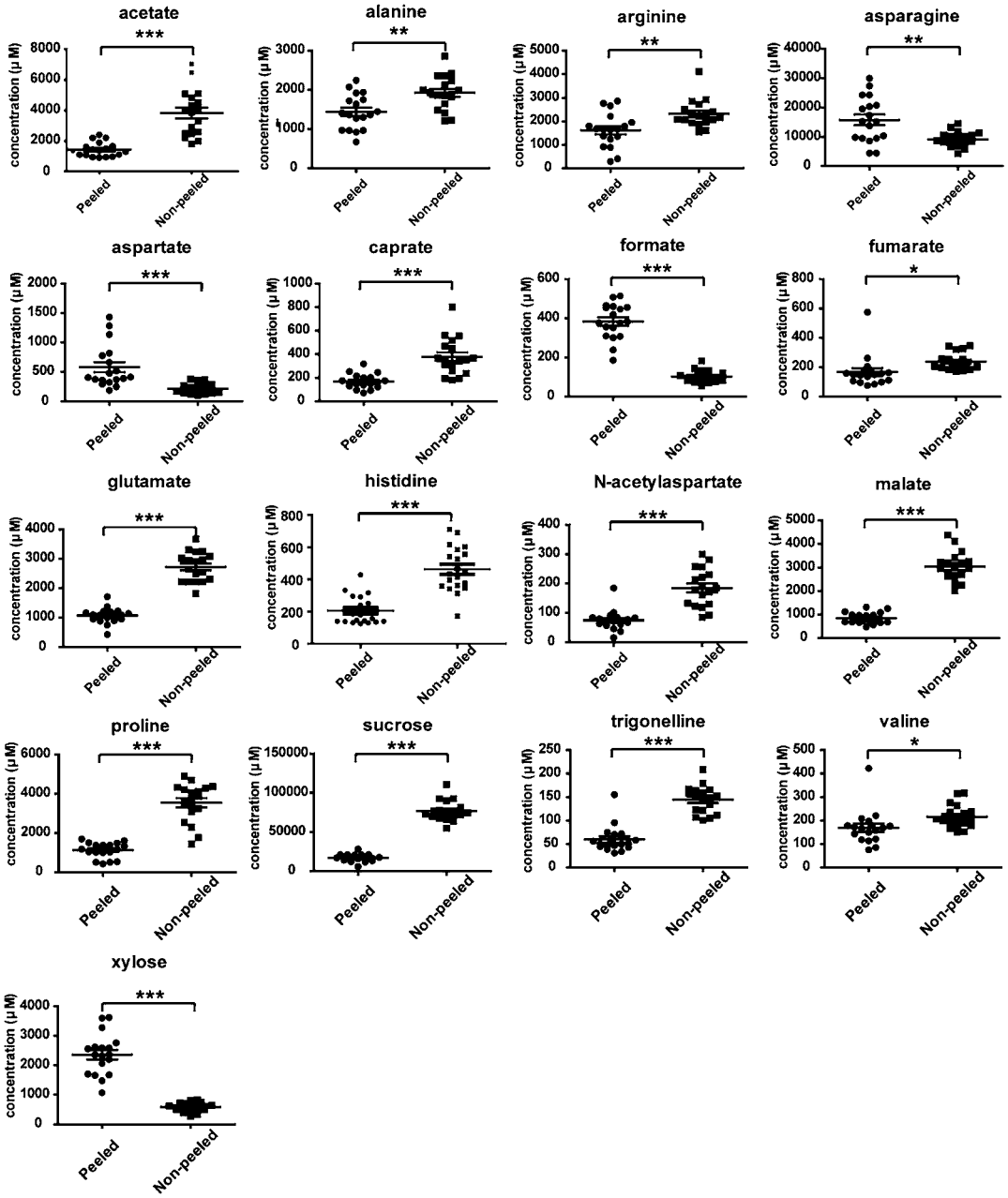

Figure 7. Quantification of metabolites indentified from the root extracts of *Astragalus* using ^{1}H NMR. *, $p < 0.05$; **, $p < 0.001$; ***, $p < 0.0001$. Student's *t* test was performed using GraphPad PRISM, and 18 samples per group were used to calculate mean and standard error.

possible carbon sources for bacteria. In addition, the major pathway of glutamate utilization in bacteroids is transamination to form aspartate followed by direct deamination of aspartate by aspartase.[32] A ureide transporter, asparagine, is the principal amino acid transported in the xylem of both nodulated and non-nodulated plants.[33,34] Therefore, peeled *Astragalus* contains relatively higher levels of aspartate and asparagine. In addition, xylose, and the precursor hemicellulose, is one of the main constituents of biomass in xylem[35] with far lower concentrations in leaves and bark. Therefore, levels of xyloses were higher in extracts of peeled *Astragalus* root.[36]

Formate, one of the higher metabolites in xylem, also has been proposed as the final signal in the transduction pathway leading to formate dehydrogenase response, the abundance of enzyme which increases greatly under various stress conditions such as drought, hypoxia, chill, dark, and wounding.[37] Therefore, levels of formate in peeled *Astragalus* roots could be increased due to the stress induced by the peeling process.

Alteration of Secondary Metabolites. On the general market, *Astragalus* roots are graded by various aspects of their physical appearance, such as root length and diameter.[38] In Korea, roots with a clean, white appearance are often graded higher and deemed more valuable. Therefore, >80% of the *Astragalus* roots cultivated in Korea are peeled prior to sale. However, for pharmacological purposes, the levels of selected active constituents, such as astragalosides and isoflavonoids, in *Astragalus* are used as the standards for quality control. High quality is indicated by higher levels of these constituents.[6,39−41]

The current study also examined secondary metabolites, which are often used to assign value to pharmacological samples, using NMR and UPLC-MS. UPLC-MS is particularly well suited for secondary metabolites. Two astragalosides and five isoflavonoids

dx.doi.org/10.1021/jf4026103 | J. Agric. Food Chem. 2013, 61, 10398−10407

Table 2. Metabolite Compound Intensities Identified by UPLC-MS

compound	mean ± standard error (area ratio)[a] peeled (n = 18)	unpeeled (n = 18)	p value[b]
Positive Mode			
calycosin-7-*O*-β-D-glucose[c]	2.24 ± 0.30	5.21 ± 0.43	<0.0001
calycosin-7-*O*-β-D-glucoside-6″-*O*-malonate[c]	4.64 ± 0.65	11.58 ± 0.90	<0.0001
calycosin[c]	7.45 ± 0.58	4.68 ± 0.40	0.003
ononin[c]	8.05 ± 1.11	10.55 ± 0.95	0.0952
formononetin	6.47 ± 0.83	1.79 ± 0.24	<0.0001
Negative Mode			
astragaloside IV	0.04 ± 0.00	0.09 ± 0.01	<0.0001
astragaloside II[c]	0.05 ± 0.01	0.17 ± 0.02	<0.0001

[a]Area ratios were calculated by dividing BEHP area in positive mode and DSS area in negative mode, respectively. [b]P values were calculated from Student's t test using GraphPad PRISM. [c]Compounds were tentatively identified using MS and MS/MS patterns.

were quantitated relative to an internal standard using UPLC-MS (Table 2).

In conventional extraction procedures, isoflavonoid glycoside malonates are typically converted into their respective glycosides or flavonoid glycons.[42] In our results, calycosin-7-*O*-β-D-glucoside-6″-*O*-malonate and calycosin-7-*O*-β-D-glucose were present at significantly higher levels in unpeeled *Astragalus*, whereas calycosin itself was significantly higher in peeled samples. In addition, although ononin, a formononetin derivate, was present at equivalent levels in unpeeled and peeled *Astragalus*, formononetin was present at higher levels in peeled *Astragalus*. These results might be indicative of the high stability of isoflavonoides in unpeeled *Astragalus* root. The triterpene saponins, astragalosides II and IV, which are also important active compounds in *Astragalus*, were found at higher levels in unpeeled roots.[43] This result agrees with the findings of Song,[6] who reported that the total astragaloside content of the bark is 74-fold higher than that in the xylem. Song's study also found no significant differences between the total isoflavonoid content of xylem and bark. Together, these results might show that while the contents of isoflavonoid glycoside malonate and isoflavonoid glycoside were higher in unpeeled roots due to their relative stability, the total isoflavonoid content did not change significantly as a result of peeling. Instead, levels of triterpene saponins were higher in the unpeeled samples. These differences may result in different levels of biological activity between peeled and unpeeled *Astragalus* roots.[5]

In this study, a complementary approach using both NMR and UPLC-MS platforms was employed to discern differences in primary and secondary metabolite levels to monitor the postharvest peeling of *Astragalus* roots. Patterns of primary and secondary metabolites in unpeeled and peeled *Astragalus* differed significantly, according to multivariate PCAs of global and targeted variables. Levels of nearly all of the primary metabolites were higher in unpeeled *Astragalus*. In particular, unpeeled *Astragalus* has high levels of arginine and valine, essential amino acids, which are not synthesized in the human body, and a high level of sucrose, which is the most accessible source of energy for the human body and spares protein from being broken down for energy.[44] However, asparagine, aspartate, and xylose, which are xylem-related compounds, and formate, which results from wound-induced stress, were higher in peeled *Astragalus*. In addition, isoflavonoid glycoside malonate in peeled *Astragalus* might be easily converted to glycosides or flavonoid glycons during the extraction procedure, and levels of astraglosides were higher in unpeeled samples.

In general, secondary metabolites including saponins, isoflavonoids, polysaccharides, and astragalosides have been known as biologically active constituents of *Astragalus* roots. Of these, unpeeled *Astragalus* roots contained higher levels of saponins, astragalosides, and polysaccharides, which have antihyperglycemic and anti-inflammatory activities.[45−48] Therefore, these results indicated that the quality of unpeeled *Astragalus* roots was higher than that of peeled *Astragalus* roots.

Postharvest processing often determines the quality of herbal medicines and root plants. Yet, an overall assessment using several complementary platforms has not been developed, and a specific platform for analyzing targeted secondary metabolites using HPLC has only been reported to data.[7,49] Therefore, the combined ^{1}H NMR and UPLC-MS analyses, coupled with chemometric analysis, can be used to ensure proper postharvest processing by providing information about primary and secondary metabolites.

■ ASSOCIATED CONTENT

Ⓢ Supporting Information

Additional experimental details, figures, and a table. This material is available free of charge via the Internet at http://pubs.acs.org.

■ AUTHOR INFORMATION

Corresponding Author

*(G.-S.H.): Korea Basic Science Institute, Seoul 136-713, Republic of Korea. Phone: +82-2-6943 4137. Fax: +82-2-6943-4108. Email: gshwang@kbsi.re.kr. (D. H. R.): Sungkyunkwan University, Suwon 440-746, Republic of Korea. Phone: +82-31-290-5931. Fax: +82-31-290-5976. E-mail: dhryu@skku.edu.

Funding

This work was supported by the National Research Foundation of Korea Grant funded by the Korean government (MSIP) (2013 University-Institute cooperation program) and the Korea Basic Science Institute (T3373B).

Notes

The authors declare no competing financial interest.

■ REFERENCES

(1) Gui, S. Y.; Wei, W.; Wang, H.; Wu, L.; Sun, W. Y.; Chen, W. B.; Wu, C. Y. Effects and mechanisms of crude astragalosides fraction on liver fibrosis in rats. *J. Ethnopharmacol.* **2006**, *103*, 154−159.

(2) Sinclair, S. Chinese herbs: a clinical review of *Astragalus*, *Ligusticum*, and *Schizandrae*. *Altern. Med. Rev.* **1998**, *3*, 338−344.

(3) Song, Z. H.; Ji, Z. N.; Lo, C. K.; Dong, T. T.; Zhao, K. J.; Li, O. T.; Haines, C. J.; Kung, S. D.; Tsim, K. W. Chemical and biological assessment of a traditional chinese herbal decoction prepared from Radix Astragali and Radix Angelicae Sinensis: orthogonal array design to optimize the extraction of chemical constituents. *Planta Med.* **2004**, *70*, 1222−1227.

(4) Zhang, X.; Feng, J.; Mu, K.; Ma, H.; Niu, X.; Liu, C.; Dang, Q. Effects of single herbal drugs on adhesion and migration of melanocytes. *J. Tradit. Chin. Med.* **2005**, *25*, 219−221.

(5) Goh, E.; Seong, E.; Lee, J.; Na, J.; Lim, J.; Kim, M.; Kim, N.; Lee, G.; Seo, J.; Cheoi, D. Antioxidant activities according to peeling and cultivated years of *Astragalus membranaceus* roots. *Korean J. Med. Crop Sci.* **2009**, *17*, 234−237.

(6) Song, J. Z.; Yiu, H. H.; Qiao, C. F.; Han, Q. B.; Xu, H. X. Chemical comparison and classification of Radix *Astragali* by determination of

isoflavonoids and astragalosides. *J. Pharm. Biomed. Anal.* **2008**, *47*, 399−406.
(7) Kwon, H. J.; Hwang, J.; Lee, S. K.; Park, Y. D. Astragaloside content in the periderm, cortex, and xylem of *Astragalus membranaceus* root. *J. Nat. Med.* **2013**, DOI: 10.1007/s11418-013-0741-8.
(8) Mahady, G. B; Fong, H. H. S.; Farnsworth, N. R. *Botanical Dietary Supplements: Quality, Safety and Efficacy*; Swets & Zeitlinger: Lisse, The Netherlands, 2001.
(9) Chan, E. C.; Yap, S. L.; Lau, A. J.; Leow, P. C.; Toh, D. F.; Koh, H. L. Ultra-performance liquid chromatography/time-of-flight mass spectrometry based metabolomics of raw and steamed *Panax notoginseng*. *Rapid Commun. Mass Spectrom.* **2007**, *21*, 519−528.
(10) Wagner, S.; Scholz, K.; Donegan, M.; Burton, L.; Wingate, J.; Volkel, W. Metabonomics and biomarker discovery: LC-MS metabolic profiling and constant neutral loss scanning combined with multivariate data analysis for mercapturic acid analysis. *Anal. Chem.* **2006**, *78*, 1296−1305.
(11) Fiehn, O.; Kopka, J.; Dormann, P.; Altmann, T.; Trethewey, R. N.; Willmitzer, L. Metabolite profiling for plant functional genomics. *Nat. Biotechnol.* **2000**, *18*, 1157−1161.
(12) Want, E. J.; Cravatt, B. F.; Siuzdak, G. The expanding role of mass spectrometry in metabolite profiling and characterization. *Chembiochem* **2005**, *6*, 1941−1951.
(13) Nordstrom, A.; O'Maille, G.; Qin, C.; Siuzdak, G. Nonlinear data alignment for UPLC-MS and HPLC-MS based metabolomics: quantitative analysis of endogenous and exogenous metabolites in human serum. *Anal. Chem.* **2006**, *78*, 3289−3295.
(14) Okazaki, Y.; Saito, K. Recent advances of metabolomics in plant biotechnology. *Plant Biotechnol. Rep.* **2012**, *6*, 1−15.
(15) Kim, E. J.; Kwon, J.; Park, S. H.; Park, C.; Seo, Y. B.; Shin, H. K.; Kim, H. K.; Lee, K. S.; Choi, S. Y.; Ryu, D. H.; Hwang, G. S. Metabolite profiling of *Angelica gigas* from different geographical origins using ^{1}H NMR and UPLC-MS analyses. *J. Agric. Food Chem.* **2011**, *59*, 8806−8815.
(16) Lee, A. R.; Gautam, M.; Kim, J.; Shin, W. J.; Choi, M. S.; Bong, Y. S.; Hwang, G. S.; Lee, K. S. A multianalytical approach for determining the geographical origin of ginseng using strontium isotopes, multielements, and ^{1}H NMR analysis. *J. Agric. Food Chem.* **2011**, *59*, 8560−8567.
(17) Lee, J. E.; Hong, Y. S.; Lee, C. H. Characterization of fermentative behaviors of lactic acid bacteria in grape wines through ^{1}H NMR- and GC-based metabolic profiling. *J. Agric. Food Chem.* **2009**, *57*, 4810−4817.
(18) Krishnan, P.; Kruger, N. J.; Ratcliffe, R. G. Metabolite fingerprinting and profiling in plants using NMR. *J. Exp. Bot.* **2005**, *56*, 255−265.
(19) Wilson, I. D.; Nicholson, J. K.; Castro-Perez, J.; Granger, J. H.; Johnson, K. A.; Smith, B. W.; Plumb, R. S. High resolution "ultra performance" liquid chromatography coupled to oa-TOF mass spectrometry as a tool for differential metabolic pathway profiling in functional genomic studies. *J. Proteome Res.* **2005**, *4*, 591−598.
(20) Shen, Y.; Zhang, R.; Moore, R. J.; Kim, J.; Metz, T. O.; Hixson, K. K.; Zhao, R.; Livesay, E. A.; Udseth, H. R.; Smith, R. D. Automated 20 kpsi RPLC-MS and MS/MS with chromatographic peak capacities of 1000−1500 and capabilities in proteomics and metabolomics. *Anal. Chem.* **2005**, *77*, 3090−3100.
(21) Pan, Z.; Raftery, D. Comparing and combining NMR spectroscopy and mass spectrometry in metabolomics. *Anal. Bioanal. Chem.* **2007**, *387*, 525−527.
(22) Duan, L. X.; Chen, T. L.; Li, M.; Chen, M.; Zhou, Y. Q.; Cui, G. H.; Zhao, A. H.; Jia, W.; Huang, L. Q.; Qi, X. Use of the metabolomics approach to characterize Chinese medicinal material Huangqi. *Mol. Plant* **2012**, *5*, 376−386.
(23) Ryu, S.; Lee, H.; Kim, Y.; Kim, S. Determination of isoprenyl and lavandulyl positions of flavonoids from Sophora flavescens by NMR experiment. *Arch. Pharm. Res.* **1997**, *20*, 491−495.
(24) Du, X.; Bai, Y.; Liang, H.; Wang, Z.; Zhao, Y.; Zhang, Q.; Huang, L. Solvent effect in ^{1}H NMR spectra of 3′-hydroxy-4′-methoxy isoflavonoids from *Astragalus membranaceus* var. *mongholicus*. *Magn. Reson. Chem.* **2006**, *44*, 708−712.
(25) Craig, A.; Cloarec, O.; Holmes, E.; Nicholson, J. K.; Lindon, J. C. Scaling and normalization effects in NMR spectroscopic metabonomic data sets. *Anal. Chem.* **2006**, *78*, 2262−2267.
(26) Pate, J. S.; Sharkey, P. J.; Lewis, O. A. M. Xylem to phloem transfer of solutes in fruiting shoots of legumes, studied by a phloem bleeding technique. *Planta* **1975**, *122*, 11−26.
(27) Gessler, A.; Kopriva, S.; Rennenberg, H. Regulation of nitrate uptake at the whole-tree level: interaction between nitrogen compounds, cytokinins and carbon metabolism. *Tree Physiol.* **2004**, *24*, 1313−1321.
(28) Gojon, A.; Passard, C.; Bussi, C. *Root/SHOOT DISTRibution of NO_3^- Assimilation in Herbaceous and Woody Species*; SPB Academic Publishing: The Hague, The Netherlands, 1994; pp 131−147.
(29) Dambrine, E.; Martin, F.; Carisey, N.; Granier, A.; Hällgren, J.-E.; Bishop, K. Xylem sap composition: a tool for investigating mineral uptake and cycling in adult spruce. *Plant Soil* **1995**, *169*, 233−241.
(30) Schmidt, S.; Stewart, G. R. Transport, storage and mobilization of nitrogen by trees and shrubs in the wet/dry tropics of northern Australia. *Tree Physiol.* **1998**, *18*, 403−410.
(31) Gessler, A.; Schneider, S.; Weber, P.; Hanemann, U.; Rennenberg, H. Soluble N compounds in trees exposed to high loads of N: a comparison between the roots of Norway spruce (*Picea abies*) and beech (*Fagus sylvatica*) trees grown under field conditions. *New Phytol.* **1998**, *138*, 385−399.
(32) Kouchi, H.; Fukai, K.; Kihara, A. Metabolism of glutamate and aspartate in bacteroids isolated from soybean root nodules. *J. Gen. Microbiol.* **1991**, *137*, 2901−2910.
(33) McClure, P. R.; Israel, D. W. Transport of nitrogen in the xylem of soybean plants. *Plant Physiol.* **1979**, *64*, 411−416.
(34) Puiatti, M.; Sodek, L. Waterlogging affects nitrogen transport in the xylem of soybean. *Plant Physiol. Biochem.* **1999**, *37*, 767−773.
(35) Suzuki, S.; Li, L.; Sun, Y.-H.; Chiang, V. L. The cellulose synthase gene superfamily and biochemical functions of xylem-specific cellulose synthase-like genes in *Populus trichocarpa*. *Plant Physiol.* **2006**, *142*, 1233−1245.
(36) Schädel, C.; Blöchl, A.; Richter, A.; Hoch, G. Quantification and monosaccharide composition of hemicelluloses from different plant functional types. *Plant Physiol. Biochem.* **2010**, *48*, 1−8.
(37) Hourton-Cabassa, C.; Ambard-Bretteville, F.; Moreau, F.; Davy de Virville, J.; Remy, R.; Francs-Small, C. C. Stress induction of mitochondrial formate dehydrogenase in potato leaves. *Plant Physiol.* **1998**, *116*, 627−635.
(38) Xu, G. J.; He, H. H.; Xu, L. S.; Jin, R. L. *The Chinese Material Medica.*; China Medico-Pharmaceutical Science & Technology Publishing House: Beijing, China, 2001; p 230.
(39) Ma, X. Q.; Shi, Q.; Duan, J. A.; Dong, T. T.; Tsim, K. W. Chemical analysis of *Radix Astragali* (Huangqi) in China: a comparison with its adulterants and seasonal variations. *J. Agric. Food Chem.* **2002**, *50*, 4861−4866.
(40) Wang, D.; Song, Y.; Li, S. L.; Bian, Y. Y.; Guan, J.; Li, P. Simultaneous analysis of seven astragalosides in *Radix Astragali* and related preparations by liquid chromatography coupled with electrospray ionization time-of-flight mass spectrometry. *J. Sep. Sci.* **2006**, *29*, 2012−2022.
(41) Dong, T. T.; Zhao, K. J.; Gao, Q. T.; Ji, Z. N.; Zhu, T. T.; Li, J.; Duan, R.; Cheung, A. W.; Tsim, K. W. Chemical and biological assessment of a chinese herbal decoction containing *Radix Astragali* and *Radix Angelicae Sinensis*: determination of drug ratio in having optimized properties. *J. Agric. Food Chem.* **2006**, *54*, 2767−2774.
(42) Li, S.; Han, Q.; Qiao, C.; Song, J.; Lung Cheng, C.; Xu, H. Chemical markers for the quality control of herbal medicines: an overview. *Chin. Med.* **2008**, *3*, 7−22.
(43) Qi, L. W.; Yu, Q. T.; Li, P.; Li, S. L.; Wang, Y. X.; Sheng, L. H.; Yi, L. Quality evaluation of *Radix Astragali* through a simultaneous determination of six major active isoflavonoids and four main saponins by high-performance liquid chromatography coupled with diode array and evaporative light scattering detectors. *J. Chromatogr., A* **2006**, *1134*, 162−169.

(44) Hounsome, N.; Hounsome, B.; Tomos, D.; Edwards-Jones, G. Plant metabolites and nutritional quality of vegetables. *J. Food Sci.* **2008**, *73*, R48−R65.
(45) Motomura, K.; Fujiwara, Y.; Kiyota, N.; Tsurushima, K.; Takeya, M.; Nohara, T.; Nagai, R.; Ikeda, T. Astragalosides isolated from the root of *Astragalus* radix inhibit the formation of advanced glycation end products. *J. Agric. Food Chem.* **2009**, *57*, 7666−7672.
(46) Wang, N.; Zhang, D.; Mao, X.; Zou, F.; Jin, H.; Ouyang, J. *Astragalus* polysaccharides decreased the expression of PTP1B through relieving ER stress induced activation of ATF6 in a rat model of type 2 diabetes. *Mol. Cell. Endocrinol.* **2009**, *307*, 89−98.
(47) Liu, M.; Wu, K.; Mao, X.; Wu, Y.; Ouyang, J. *Astragalus* polysaccharide improves insulin sensitivity in KKAy mice: regulation of PKB/GLUT4 signaling in skeletal muscle. *J. Ethnopharmacol.* **2010**, *127*, 32−37.
(48) Gao, X. H.; Xu, X. X.; Pan, R.; Li, Y.; Luo, Y. B.; Xia, Y. F.; Murata, K.; Matsuda, H.; Dai, Y. Saponin fraction from *Astragalus membranaceus* roots protects mice against polymicrobial sepsis induced by cecal ligation and puncture by inhibiting inflammation and upregulating protein C pathway. *J. Nat. Med.* **2009**, *63*, 421−429.
(49) Mäder, J.; Rawel, H.; Kroh, L. W. Composition of phenolic compounds and glycoalkaloids α-solanine and α-chaconine during commercial potato processing. *J. Agric. Food Chem.* **2009**, *57*, 6292−6297.